ORIGINAL ARTICLE

WILEY

Carboxymethyl chitosan bounded iron oxide nanoparticles and gamma-irradiated avian influenza subtype H9N2 vaccine to development of immunity on mouse and chicken

Farahnaz Motamedi-sedeh[1] | Atefeh Saboorizadeh[2] | Iraj Khalili[3] |
Massomeh Sharbatdaran[4] | Viskam Wijewardana[5] | Arash Arbabi[6]

[1] Department of Veterinary and Animal Science, Nuclear Agriculture Research School, Nuclear Science and Technology Research Institute, Karaj, Iran

[2] Department of Microbiology, Science Faculty, Islamic Azad University, Karaj Branch, Karaj, Iran

[3] Razi Vaccine and Serum Research Institute, Agricultural Research, Education and Extension Organization, Karaj, Iran

[4] Physics and accelerator Research School, Nuclear Science and Technology Research Institute, Tehran, Iran

[5] Department of Nuclear Sciences and Applications, Animal Production and Health Section, International Atomic Energy Agency (IAEA), Vienna International Centre (VIC), Vienna, Austria

[6] Faulty of Medical Science, Tehran University of Medical Science, Tehran, Iran

Correspondence
Farahnaz Motamedi-sedeh, Nuclear Science and Technology Research Institute, Tehran, Iran.
Email: farah.motamedi@gmail.com; fmotamedi@aeoi.org.ir

Abstract

Background: Avian influenza virus (AIV) subtype H9N2 is a low pathogenic avian influenza virus (LPAIV).

Objective: This study aims to evaluate the humoral and cellular immunity in vaccinated mice and broiler chicken by irradiated AIV antigen plus carboxymethyl chitosan bounded iron oxide nanoparticles (CMC-IO NPs) as an adjuvant.

Methods: AIV subtype H9N2 with $10^{8.5}$ EID_{50}/ml and haemagglutinin antigen assay about 10 $\log_2$ was irradiated by 30 kGy gamma radiation dose. Then, the gamma-irradiated AIV was used as an inactivated vaccine and conjugated with CMC-IO NPs to improve immune responses on mice. IO NPs must be applied in all activated tests using 1-ethyl-3-(3-dimethylaminopropyl) carbodiimide (EDC) and N-hydroxysulfosuccinimide sodium salt (sulfo-NHS), and then functionalized by CMC as IO-CMC. Fourier transform infrared (FTIR) spectra on functionalized IO-CMC showed a peak of 638 cm^{-1} which is a band between metal and O (Fe-O).

Results: Based on the comparison between the two X-ray diffraction (XRD) patterns on Fe_2O_3-NPs and IO-CMC, the characteristics of IO-NPs did not change after carboxymethylation. A CHN Analyzer was applied to measure the molecular weight of IO-CMC that was calculated as 1045 g. IO-CMC, irradiated AIV-IO-CMC and formalin AIV-IO-CMC were injected into 42 BALB/c mice in six groups. The fourth group was the negative control, and the fifth and sixth groups were inoculated by irradiated AIV-ISA70 and formalin AIV-ISA70 vaccines. An increase in haemagglutination inhibition (HI) antibody titration was observed in the irradiated AIV-IO-CMC and formalin AIV-IO-CMC groups ($p < 0.05$). In addition, increases in the lymphoproliferative activity of re-stimulated splenic lymphocytes, interfron-γ (IFN-γ) and interleukin-2 (IL-2) concentration in the irradiated AIV-IO-CMC group demonstrated the activation of Type 1 helper cells. The concentration of IL-4 was without any significant increases in non-group.

Conclusions: Accordingly, Th2 activation represented no increase. Finally, the finding showed that AIV-IO-CMC was effective on enhancing immunogenicity as irradiated AIV antigen administered with a clinically acceptable adjuvant (i.e. IO-CMC).

1 | INTRODUCTION

Avian influenza virus (AIV) belongs to the influenza A genus. Influenza A viruses have different subtypes based on haemagglutinin (HA) and neuraminidase (NA) surface antigens. AIVs are categorized into two groups of high and low pathogenic based on the disease in poultry. Highly pathogenic avian influenza viruses (HPAIV) result in high mortality in some poultry species. Low pathogenic avian influenza viruses (LPAIV) also cause outbreaks in poultry but are not associated with severe disease (Peacock et al., 2019). H9N2 is an LPAIV subtype which is found in wild birds and poultry worldwide, and these viruses have mono-, di-, or tri-basic cleavage sites in the HA antigen by extracellular trypsin protease causing LPAIV to restrict respiratory and gastrointestinal tracts, where these proteases are expressed (Peacock et al., 2019, Parvin et al., 2020). The vaccination of poultry against H9N2 is routinely used to control this endemic disease in large areas of Asia (Ghadimipour et al., 2014). Given the antigenic variations in the influenza virus, designing a new vaccine that induces a high protective immune response is considered essential (Alsharifi et al., 2009; Motobu et al., 2002). It is shown that gamma-irradiated influenza A virus (γ-Flu) as a vaccine is effective in this regard. It can induce that T-cell response provides and has cross-protective immunity against seasonal and pandemic influenza virus (Alsharifi et al., 2009; Khalil et al., 2015). Gamma irradiation is the perfect method for virus inactivation science, and it has high penetration while a slight effect on the antigenic construction and breaks the RNA strand of the virus (Alsharifi & Müllbacher, 2010). Further, adjuvants often influence the quality of the immune responses in different ways; thus, new strategies are required for expanding the vaccine adjuvants and delivery systems. Nanoparticles (NPs) can be used as a delivery system for improving immunogenicity of vaccines. Although metallic NPs have been tested as drug delivery, limited attempts have been made to apply these NPs as vaccine platforms (Pusic et al., 2013). The size of NPs is important for tissue penetration and facilitates reaching immunological organs. Iron oxide (IO, Fe_2O_3) NPs have been recently employed in several medical applications such as magnetic resonance imaging contrast agents (super-paramagnetic IO NPs) and the detection of lymph node metastasis (Anzai, 2004; Figuero, 2010). IO NPs could be utilized as a new adjuvant for immunization against AIV because of some of their characteristics such as having safety profiles, being water-soluble, being applied as a drug delivery system and having low-cost production (Xu et al., 2010; Xu, Aguilar, et al. 2009; Xu, Wei, et al. 2009). In this study, IO NPs were coated with carboxymethyl chitosan (CMC) so that the car-boxylate groups could be conjugated with viral surface proteins. Then, the gamma-irradiated AIV subtype H9N2 as an inactivated vaccine was conjugated with CMC bounded Fe_2O_3 (CMC-Fe_2O_3) NPs and used to immunize on BALB/c mice.

2 | MATERIALS AND METHODS

2.1 | Virus and vaccines

Razi Vaccine and Serum Research Institute of Iran received the AIV subtype H9N2 strain (A/Chicken/IRN/Ghazvin/2001) as a gift for this study. According to the procedure described by Salehi et al. (2018), the optimum gamma irradiation dose was used to inactivate virus samples. First, the AIV was multiplied on embryonated specific free pathogen (SPF) chicken eggs, and then the HA antigen of irradiated and non-irradiated viral samples was analyzed by haemagglutination test (HAT) as the pattern method of the World Health Organization (Health, 2015; Pourbakhsh et al., 2004; STEAR, 2005; WHO, 2013). The virus titration was calculated via the embryo-infective dose (EID_{50}) of infected allantoic fluid according to the method of Reed and Muench (1938). A gamma-ray dose of 30 kGy was recommended for the complete inactivation of frozen AIV subtype H9N2 samples (Salehi et al., 2018). Infectivity of irradiated virus samples was determined by eggs inoculation method during four blind cultures on embryonated SPF chicken eggs of 9–11 days for safety test, and virus titration was obtained by EID_{50} methods. The frozen AIV subtype H9N2 was irradiated by an instrument (model 220, gamma cell; Nordion Company, Canada) at a dose rate of 2.07 Gy/s and activity of 8677 Ci for virus inactivation on dry ice. Gamma-irradiated AIV was used as an irradiated inactivated vaccine. Formalin vaccine was prepared by Razi protocol. Briefly, AIV was inactivated by a formalin concentration of 0.1% at 25°C for 24 h and applied as formalin-vaccine (Raie Jadidi et al., 2017). The formalin-inactivated AIV and irradiated AIV were formulated as conventional (commercial) and irradiated vaccines by Montanide Oil (ISA70), respectively. Both formalin-treated and -irradiated AIVs were formulated by CMC magnetic NPs as new adjuvant.

2.2 | Synthesis of carboxymethyl chitosan magnetic nanoparticles (CMC-IO)

CMC preparation included slow addition of 1.3 g chitosan and 2 g NaOH to 27 ml deionized water: isopropanol mixture (1:3.5 ratio)

under stirring for 1 h. Then, 3 ml of isopropanol containing 1.6 g monochloroacetic acid solution was added to the reaction mixture in drops in 1 h. After reacting for 4 h at room temperature (RT), 25 ml of ethanol 70% was added to stop the reaction. The solid product was filtered and washed with 80% ethanol twice and dried at RT (Mourya et al., 2010; Pusic et al., 2013). This product is CMC used for the bio-functionalization of Fe_2O_3-NPs. Briefly, 10 ml deionized water was added to 100 mg IO (Fe_2O_3)-NPs (Teconan Company) with various diameters (i.e. 20–30 nm). In addition, the pH level was adjusted by NaOH (0.1 M) to about 8, and an ultrasonic device was used to disperse the mixture for 20 min. Then, 0.3 g CMC was added and again the ultrasonic device was used for 30 min, and stirred for 12 h. After adding 10 ml deionized water and ultrasonic waves for 5 min, the CMC magnetic NPs were separated by magnetic-iron and washed with deionized water and ethanol twice. The CMC magnetic microspheres were dried for 48 h at RT and hit in a mortar to be crushed into a powder (Pusic et al., 2013; Xie et al., 2014). Fourier transform infrared (FTIR) spectroscopic measurements were performed by PerkinElmer spectrum100 instrument (USA) on CMC and IO-CMC. The wave numbers of the FTIR measurement range were controlled from 450 to 4000 cm^{-1} (Asgari et al., 2014). The X-ray diffraction (XRD) pattern was performed by an XRD (STOE STADI-MP) diffractometer on IO (Fe_2O_3) NPs and IO-CMC complex (Xie et al., 2014). A CHN Analyzer (a carbon, hydrogen and nitrogen analyzer, The PerkinElmer 2400 Series II CHNS/O Elemental Analyzer) was used to measure carbon, hydrogen and nitrogen elemental concentrations in IO-CMC, along with calculating the molecular weight of IO-CMC (Asgari et al., 2014).

2.3 | Conjugation of CMC-IO (AIV-IO-CMC)

Irradiated AIV and formalin-inactivated AIV were frozen and thawed thrice and centrifuged at 5000 g at 4°C for 15 min. Then, supernatant was separated and the protein concentration of the plate was measured by NanoDrop (Smart-Nano, Canada). Irradiated AIV and formalin-treated antigen were conjugated by IO-CMC that was prepared in-house using sulfo-NHS and 1-ethyl-3-(3-dimethylaminopropyl) carbodiimide (EDC) covalent coupling chemistry. Briefly, IO-CMC (100 mg) was activated by adding and incubating sulfo-NHS (5.5 mg, molar ratio 2000:1) and EDC (9 mg, molar ratio 2000:1) for 5 min in 20 ml sterile borate buffer (NaCl 2.5 g, disodium tetra borate 2.85 g, boric acid 10.5 g and deionized water 1000 ml) with a pH value of 7.4. Next, 5 ml of irradiated AIV and formalin-treated AIV were added, thoroughly vortexed and reacted overnight at 2–8°C. Finally, the reaction was quenched by adding 100 μl of quenching buffer (Tris-HCl 0.1 M and pH 7.5) and mixed for 10 min at RT. The irradiated AIV and formalin-treated AIV conjugated with IO-CMC were purified/separated using the magnetic separator overnight at 4°C. Then, the supernatant was removed and IO NPs were re-suspended in 5 ml phosphate buffered saline (PBS) with vortex or sonication (Pusic et al., 2013). The irradiated AIV-CMC-IO, formalin-treated AIV-IO-CMC conjugates and unconjugated IOs were evaluated by agarose (1.5%) gel electrophoresis in tris-acetate-EDTA buffer (TAE,

pH 8.5). In each well, 10 μl of the sample (three samples were used including irradiated AIV-IO-CMC, formalin-treated AIV-IO-CMC and IO-CMC) was mixed with 5 μl of 5× TAE loading buffer (25% glycerol, 0.25% Orange G, pH 8.5). The gel was run at 100 V for 30 min, and then imaged by a gel imaging system.

2.4 | Transmission electron microscopy

The AIV was multiplied on embryonated SPF chicken eggs and concentrated by pelleting (20,000 × g for 2 h) re-suspended in HEPES, and then conjugated by IO-CMC for electron microscopy study. According to the diameter of the AIV (about 80 nm), the particle with a diameter of 80 nm should be the AIV particles (Figure 3a). Next, the concentrated virus sample was stained by a 2% heavy metal salt solution with high mass density (e.g., phosphotungstic acid). A copper grid (carrier network) was placed on a drop of the suspension. The grid carried a stable and highly electron transparent plastic carrier (formvar) film with regularly dispersed holes. After short adsorption, the sample excess and interfering ions were removed with filter paper, and the grid with the adsorbed material is placed for a few seconds on the contrast medium, which consisted of a 2.0% heavy metal salt solution with high mass density, such as phosphotungstic acid. Excess contrast medium was removed from the 'contrasted' grid, briefly air-dried and was then prepared for electron-microscopic examination (Harris et al., 2006). Transmission electron microscopy (TEM; Philips cm30) was used for analysis of morphology and size of the conjugated AIV-IO-CMC particles by negative staining method. Also, according to the data sheet iron oxide (Teconan company), the particles with 30 nm diameter are the IO particles that are coated by CMC as a cloudy cover on NPs (Figure 3b).

2.5 | Mice vaccination

Forty-two BALB/c mice with the age of about 5 weeks were purchased from Razi Vaccine and Serum Research Institute of Iran, transferred to Nuclear Agriculture Research School in Karaj and divided in six groups of seven animals each. The first group was vaccinated by irradiated AIV-IO-CMC, and formalin-treated AIV-IO-CMC was used to immunize the second group. IO-CMC was injected to the third group, and the fourth group was injected by sterile PBS as the negative control. Furthermore, the irradiated AIV plus ISA70 was injected into the group five, and finally group six was injected by formalin-treated AIV plus ISA70. Vaccination was performed intradermally on the neck of mice in two doses with an interval of 14 days.

2.6 | Immune responses of mice

Forty-two mice blood samples were collected 2 weeks after the second vaccination, and the sera were separated by low-speed centrifugation and used for the antibody titration by the haemagglutination
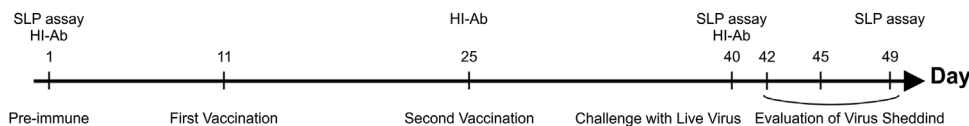
FIGURE 1 The broiler chicken vaccination diagram. Abbreviations: HI-Ab, HI-antibody titration; SLP, splenic lymphocyte proliferation

inhibition (HI) test (Health, 2015; Raie Jadidi et al., 2017). Moreover, cellular immunity was measured by the splenic lymphocyte proliferation assay (Motobu et al., 2002; Sandbulte & Roth, 2004). Briefly, the 42 spleens of the immunized mice were aseptically removed 2 weeks after the boost immunization, and the single splenic lymphocyte suspensions were prepared and incubated in 96-well plates by RPMI 1640 + 10% fetal calf serum at 37° in 5% CO_2. The cells were stimulated by irradiated inactivated AIV (3 μl/well) in triplicate. The supernatants of splenic cells were collected 48 h post-stimulation to assess interleukin-2 (IL-2) and 4 and interferon-gamma production using an eBioscience Mouse interferon (IFN)-γ, IL-2 and IL-4 ELISA kits. In addition, the spleen lymphocyte proliferation assay was conducted by the Cell Proliferation MTT kit (Roche) according to the manufacturer's instructions. Then, the absorbance was detected at 540 nm and the stimulation index (SI) was calculated for each sample (SI = mean of optical density (OD) for stimulated wells/mean of OD un-stimulated wells) (Motobu et al., 2002; Sandbulte & Roth, 2004).

2.7 | Challenge test on broiler chicken

Fifty-four broiler chickens (1 day) were purchased from Alborz Hatchery Center and divided into six groups (similar to the mice groups in Section 3.5) each including nine chickens. The route of administration was subcutaneously (SC) on the neck of the chicken. Two doses of vaccines were injected as prime and booster doses with a 2-week interval (on the 11th and 25th days). The challenge was performed with 50 μl of live virus ($10^{8.5}$ EID_{50}/ml) intranasal and ocular on 40th day. The blood samples were collected on the first day from some chickens as pre-immune sera. Similarly, the blood samples were collected on 25th (before second vaccination) and 40th (before challenge) days. The blood samples were collected on 1st, 25th and 40th days, 18 samples each day. A total of 54 blood samples were collected. The splenic lymphocyte proliferation assay was conducted on chickens on the first day for pre-immune chickens and on the 40th and 49th days by MTT test, 18 samples each day. A total of 54 spleen samples were used for culturing splenic cells. The tracheal and cloacal swap samples were collected on the 40th, 42th (2 days after the challenge), 45th and 49th days for the evaluation of virus shedding by quantitative polymerase chain reaction (qPCR), 36 swabs each day. A total of 144 tracheal swabs and 144 cloacal swabs were collected from the broiler chicken vaccination diagram, as shown in Figure 1. The real time PCR tests were performed by specific primers for the AIV H9 gene (Accession numbers of HA Gen in NCBI: FJ794817.1). Briefly, for virus gene (H9) quantitation, the cDNA of all samples was amplified using QPCR Mix Eva-Green kit (Bio & Sell, Germany), according to the manufacturer's protocol. The reaction mixture contained; 100 nM of each specific primer pair for H9 gene (F: 5′-CTACTGTTGGGAGGAAGAGAATGGT-3′, and R: 5′-TGGGCGTCTTGAATAGGGTAA-3′), 5 × QPCR mix EvaGreen (4 μl), cDNA as a template (5 μl) and up to 20 μl water (Shabat et al., 2010; Ward et al., 2004). The reaction was done at initial incubation temperature 94°C for 3 min, then 40 three-step cycles (30 s at 94°C for denaturation, 30 s at 58°C for annealing, and 30 s at 72°C for elongation) by Rotor-Gene Q (QIAGEN) system.

2.8 | Statistical analysis

The analysis of variance (one-way ANOVA) followed by the least significant difference test was used for statistical analysis. Differences were considered to be statistically significant at $p < 0.05$.

3 | RESULTS

The virus titration was calculated to be $10^{8.5}$/ml EID_{50}, and haemagglutinin antigen assay for irradiated and non-irradiated avian influenza A subtype H9N2 virus samples were obtained about 10 Log_2. Thus, the antigenicity of the HA antigen did not change in irradiated AIV. The, D_{10} value and inactivation dose of gamma radiation were 3.4 and 30 kGy, respectively. The safety test was conducted for irradiated AIV H9N2 (at 30 kGy) on SPF eggs by four blind cultures and the obtained data demonstrated no virus multiplication. The XRD patterns of magnetic Fe_2O_3-NPs and IO-CMC nanocomposites are displayed in Figure 2. The size of IO-NPs and IO-CMC were about 20 nm and 22 nm, respectively. Based on the comparison of the two XRD patterns, the characteristics of IO-NPs did not change after carboxymethylation.

FTIR spectra for CMC and functionalized Fe_2O_3 NPs-CMC were evaluated (Figure 3a–b), and the basic characteristic peaks of chitosan are at 3435 cm^{-1} (O-H stretch), 2926 cm^{-1} (C-H stretch) in two spectra. The peak at 1623 cm^{-1} (C = O band) is in two spectra, but it is more clearly seen in Figure 3b. The peak 638 cm^{-1} in the functionalized IO-CMC NPs showed a band between metal and O (Fe-O), this peak was not observed in CMC spectra. CHN analysis revealed that the amount of nitrogen in the IO-CMC is approximately 1.09%. In addition, there is only one atom of N in one molecule of CMC ($C_8H_{13}NO_7$); thus, one molecule of CMC and five molecules of IO can be banded with each other. The molecular weight of IO-CMC was calculated to be nearly 1045 g (235 + (162 × 5)). The TEM images of the coated Fe_2O_3 NPs with CMC and conjugated and inactivated AIV with IO-CMC are shown in Figure 4a–b. The virus particles surrounded by IO-CMC can be observed in Figure 3a.
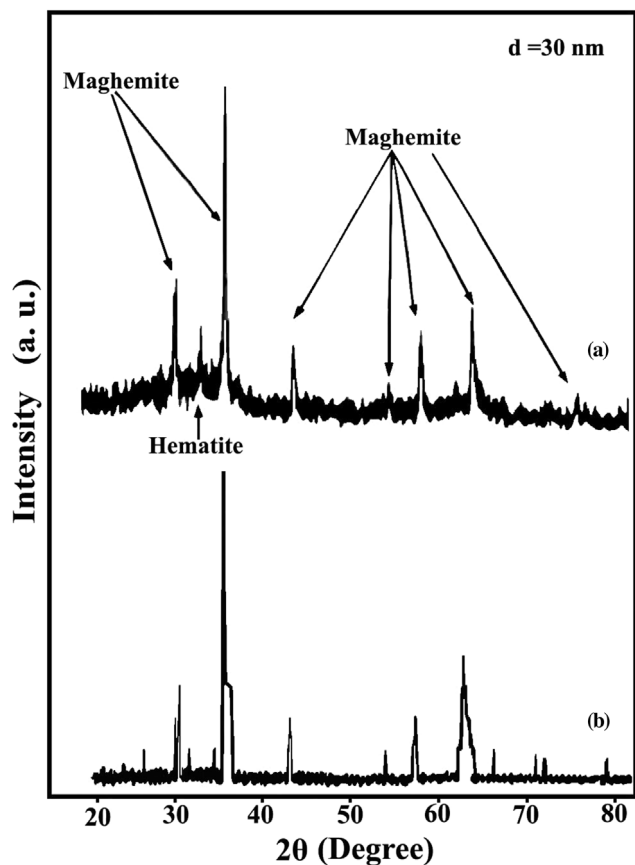
FIGURE 2 Comparison of the X-ray diffraction (XRD) patterns for iron oxide (IO) and IO-carboxymethyl chitosan (CMC) did not show any change after carboxymethylation: (a) XRD pattern for IO and (b) XRD pattern for IO-CMC
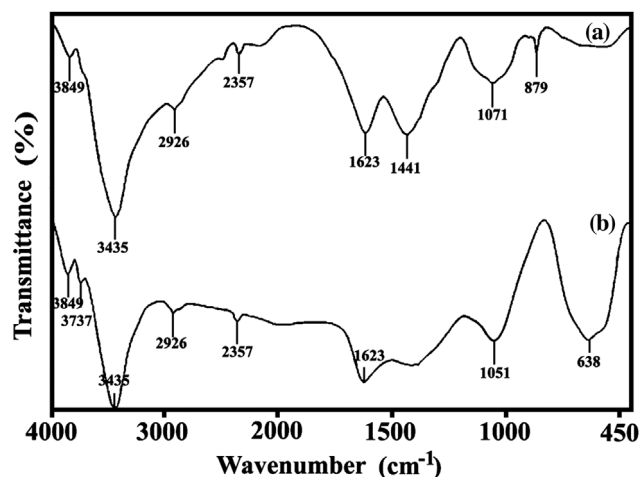

FIGURE 3 Comparison of the Fourier transform infrared (FTIR) spectra for carboxymethyl chitosan (CMC) and iron oxide (IO)-CMC, the peak 638 cm^{-1} in IO-CMC nanoparticles (NPs) showed a band between metal and O (Fe-O); this peak is not observed in CMC spectra: (a) FTRI for CMC and (b) FTRI for IO-CMC

The protein concentration of irradiated AI antigen and formalin-treated AI antigen as measured by Nanodrop are 22.1 and 26.5 $\mu g/\mu l$, respectively. Figure 5 illustrates the findings of agarose (1.5%) gel electrophoresis for evaluating the irradiated AIV-CMC-IO conjugate, AIV antigen and unconjugated IO-CMC NPs implying that conjugation was performed successfully.

The viability percentage of mice splenic cells was measured by trypan blue 2% and calculated in six vaccinated mice groups; 92.5%, 92%, 95.3%, 92.1%, 93.5% and 93%, respectively. The SI of the mice splenic cells was calculated for each sample, and the means of the obtained data are presented in Table 1. The statistical analysis of SI data represented a significant increase of the lympho-proliferative activity of re-stimulated spleen cells in the irradiated AIV-IO-CMC group ($p < 0.05$). Further, an increase was observed in mice HI antibody titration in irradiated AIV-IO-CMC and formalin-treated AIV-IO-CMC groups ($p < 0.05$). Furthermore, the increase in IFN-γ and IL-2 concentrations in the irradiated AIV-IO-CMC group revealed that Th class I cells were activated more than the other groups, leading to B-cell activation and T-cytotoxic activation. The concentration of IL-4 demonstrated no significant increases in the groups. Therefore, Th class II activation represented no increase.

The immune responses of the vaccinated broiler chicken are provided in the Table 2. Based on the findings, SI and HI antibody titration at 1st day, all of the broiler chickens were without parental immunity against AIV subtype H9N2. The HI antibody titration significantly increased in groups 1, 2, 5 and 6 chicken ($p < 0.05$) 2 weeks after the first vaccination (WAFV) at 25th day. It also represented a significant increase 2 weeks after the second vaccination (WASV) as well at 40th day. The HI antibody titration two WAFV was significantly less than two WASV ($p < 0.05$). For this reason, the vaccination was done as prime and boost strategy. The increasing of splenic lymphocyte proliferation (SI) in the 1 and 5 groups at 40th and 49th days indicated that the irradiated AIV antigen could induce the cellular immunity more than formalin-treated AIV antigen. Furthermore, the splenic lymphocyte proliferation (SI) increased in 1, 5 and 6 groups significantly ($p < 0.05$). According to the standard curve of qPCR findings from tracheal and cloacal swab samples, the virus shedding was not detected (UND) in groups 1, 2, 5 and 6 chicken at 2, 5 and 9 days after challenging with live virus. Therefore, irradiate-AIV-IO-CMC, formalin-AIV-IO-CMC, irradiated-AIV-ISA70 and formalin-AIV-ISA70 vaccines protect broiler chickens against AIV subtype H9N2.

4 | DISCUSSION

Chemical inactivation such as formalin inactivation has some toxic residues in vaccine products. Additionally, some viruses may escape during the chemical inactivation. The most commonly used chemical substances for producing inactivated vaccines can damage antigenic epitopes, leading to a reduction in immunogenicity. Gamma-ray is ionizing radiation which is emitted from Cobalt-60 isotope and used for virus inactivation without any changes in viral proteins. In general, the optimum dose of gamma radiation for virus inactivation mainly relies
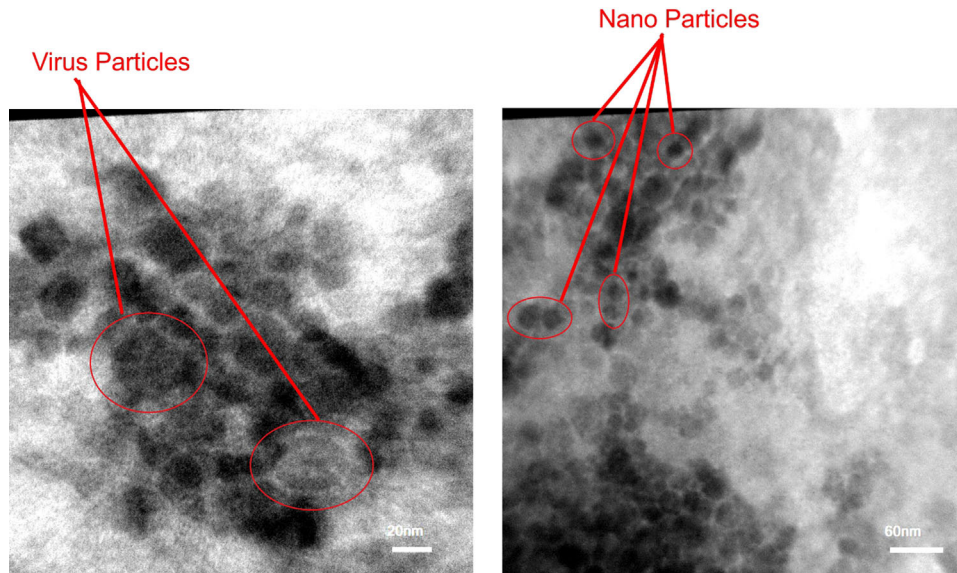
FIGURE 4 The transmission electron microscopy (TEM) images of avian influenza virus carboxymethyl chitosan bounded iron oxide (AIV-CMC-IO) conjugate and unconjugated IO-CMC nanoparticles (NPs): (a) conjugated and inactivated AIV with IO-CMC and (b) coated Fe_2O_3 NPs with CMC (IO-CMC)
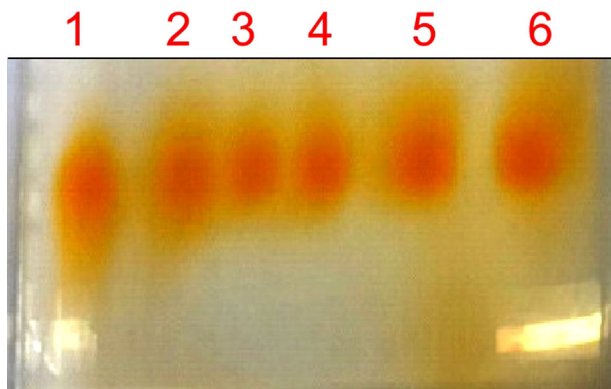

FIGURE 5 The findings of agarose (1.5%) gel electrophoresis by Orange G for evaluating the irradiated avian influenza virus carboxymethyl chitosan bounded iron oxide (AIV-CMC-IO) conjugate and unconjugated IO-CMC nanoparticles (NPs) based on molecular weight; Lane 1, AIV antigen; Lanes 2, 3 and 4, IO-CMC; Lane 5, the conjugated IO-CMC by formalin AIV antigen; Lane 6, the conjugated IO-CMC by irradiated AIV antigen

on the temperature of radiation, size and structural arrangement of the viral genome, the presence of oxygen during the irradiation process, water content and post-irradiation conditions (da Silva Aquino, 2012; Whitby & Gelda, 1979). Gamma radiation is the perfect method for virus inactivation. Due to this, vaccine preparation has a little effect on the antigenic construction, higher penetration and the ability to be used in a frozen condition that decreases free radical damage due to water radiolysis (David et al., 2017; Furuya et al., 2010; Stauffer et al., 2006). A sterility assurance level (SAL) is mathematically derived and defines the viable viral load on the final product (vaccine) after sterilization. SAL is normally expressed as 10^{-6} /ml for injectable prod-

ucts. The sterilization dose is the minimum necessary dose for achieving the required SAL. Sterilization dose depends on the first titration of viable viral load, D_{10} Value and SAL, which are required for the product (da Silva Aquino, 2012; Whitby & Gelda, 1979). There is no single adjuvant formulation to affect the quality of the immune responses against all vaccines. Recent strategies have been developed for improving immunogenicity based on NP-mediated delivery systems (Pusic et al., 2013; Reed et al., 2013). The appropriate adjuvants for vaccines are highly important for the development of innate and protective responses to combat viral diseases. They can enhance humoral and cellular immune responses while decreasing vaccine doses and prolonging immune responses (Marques Neto et al., 2017). NPs have been recently interested in drug and vaccine delivery due to their physical properties and nanosizes (Cristina et al., 2016; Langer, 1990; Orive et al., 2003; Mashhadizadeh & Amoli-Diva, 2012). Metallic NPs are synthesized by a simple method and have rigid structures. Some of these NPs have been studied for their immunological attributes (Hofmann-Amtenbrink et al., 2015; Marques Neto et al., 2017;). IO NPs have been evaluated as adjuvants by co-administration with the vaccine. Iron is an important ion in the homeostasis of all cells and the generation of immune responses. The use of IO NPs in BALB/c mice showed the diminishing of splenocyte cytokine production due to the immunomodulatory capacity of these NPs. IO NPs induce antigen presenting cell activation by inducting IL-6, tumour necrosis factor α (TNFα), IFN-γ and IL-12 production. However, the immune response, which is induced by IO NPs, is lower than the one that is generated by lipopolysaccharide (LPS) (as positive control), and it is probably beneficial for controlling the side effects (Marques Neto et al., 2017; Pusic et al., 2013). The properties and applications of CMC are strongly dependent on its structural characteristics, mainly including the average degree of substitution and the locus, amino or hydroxyl groups of the carboxymethylation

TABLE 1 The results of stimulation index of the spleen lymphocyte proliferation assay (SI), haemagglutination inhibition (HI) antibody titres, interfron-γ (IFN-γ), interleukin-2 (IL-2) and IL-4 concentration in vaccinated mice serum (In each column a>b, b>c, c>d)

No.	Vaccine group	SI ± SD	Ab titration (Log$_2$) ± SD	IFN-γ ± SD(pg/ml)	IL2 ± SD(pg/ml)	IL4 ± SD(pg/ml)
1	Irradiate-AIV-IO-CMC	1.3 ± 0.26[a]	8.18 Log$_2$ ± 2.03[a]	123.14 ± 11.75[a]	28.24 ± 1.16[a]	0.28 ± 0.056[a]
2	Formalin-AIV-IO-CMC	0.99 ± 0.15[b]	7.04 Log$_2$ ± 1.31[a]	78.15 ± 3.58[b]	16.793 ± 0.12[b]	0.22 ± 0.028[a]
3	IO-CMC	0.98 ± 0.14[b]	1.6 Log$_2$ ± 0.34[c]	17.10 ± 3.11[d]	5.605 ± 0.24[c]	0.235 ± 0.014[a]
4	PBS	0.95 ± 0.20[b]	1 Log$_2$ ± 0.75[c]	15.08 ± 2.45[d]	3.92 ± 0.71[c]	0.192 ± 0.032[a]
5	Irradiated-AIV-ISA70	1.16 ± 0.12a	5.3 Log$_2$ ± 1.15[b]	26.56 ± 2.04[c]	15.17 ± 0.16[b]	0.31 ± 0.054[a]
6	Formalin-AIV-ISA70	0.99 ± 0.06[b]	4.42 Log$_2$ ± 0.97[b]	23.01 ± 1.41[c]	11.84 ± 0.54[b]	0.30 ± 0.042[a]

Abbreviation: PBS, phosphate buffered saline.

TABLE 2 The results of chicken splenic lymphocyte proliferation (SI) and haemagglutination inhibition (HI) antibody titration in vaccinated broiler chickens

No.	Vaccine group	SI ± SD 1st day	SI ± SD 40th day	SI ± SD 49th day	Ab titration (Log$_2$) ± SD 1st day	Ab titration (Log$_2$) ± SD 25th day	Ab titration (Log$_2$) ± SD 40th day
1	Irradiate-AIV-IO-CMC	0.90 ± 0.26[a]	1.88 ± 0.21[a]	1.76 ± 0.08[a]	<1 Log$_2$[a]	2.66 Log$_2$[a]	7 Log$_2$[a]
2	Formalin-AIV-IO-CMC	0.90 ± 0.15[a]	1.12 ± 0.36[c]	1.10 ± 0.11[c]	<1 Log$_2$[a]	2.33 Log$_2$[a]	6.66 Log$_2$[a]
3	IO-CMC	0.88 ± 0.14[a]	0.91 ± 0.17[c]	0.88 ± 0.05[c]	<1 Log$_2$[a]	<1 Log$_2$[c]	< 1 Log$_2$[c]
4	PBS	0.85 ± 0.20[a]	0.94 ± 0.06[c]	0.87 ± 0.09[c]	<1 Log$_2$[a]	<1 Log$_2$[c]	< 1 Log$_2$[c]
5	Irradiated-AIV-ISA70	0.86 ± 0.12[a]	1.56 ± 0.34[a]	1.57 ± 0.23[a]	<1 Log$_2$[a]	1.66 Log$_2$[b]	5.33 Log$_2$[a]
6	Formalin-AIV-ISA70	0.89 ± 0.06[a]	1.33 ± 0.22[b]	1.38 ± 0.31[b]	<1 Log$_2$[a]	1.66 Log$_2$[b]	5 Log$_2$[b]

Abbreviation: PBS, phosphate buffered saline.

(Abreu & Campana-Filho, 2005). CMC in comparison with other water-soluble chitosan derivatives has received further attention due to ample of application, simple synthesis and an ampholytic character (Mourya et al., 2010). Pusic et al. (2013) reported no toxic effects on monkeys after three doses IO NPs injection, and thus predicted that the rapid clearance of these NPs (20 nm) should rely on their small sizes. However, more sensitive studies are needed for tracing the clearance of IO NPs. To maintain the maximum integrity of viral proteins, gamma-rays should be limited to the minimum required dose for complete inactivation of the virus. In this regard, it was found that there is a mathematical log linear-relationship ($Y = 7.95 − 0.283X$) between augmented radiation doses and diminished virus titre that is used for the assessment of D_{10} value of 3.34 kGy and the minimum inactivation dose of 30 kGy (Salehi et al., 2018). Based on the lack of detectable cytophatic effects (CPE) for all four passages and the retaining of most viral protein integrity confirmed with HAT assay, 30 kGy of gamma-irradiated AIV was used for the whole inactivated virus vaccine preparation. In the study by Salehi et al. (2018), the antigenicity of the frozen AIV after irradiation on dry ice was unaltered; thus, it was a good candidate for immunization. According to the data in Table 1, all vaccinated mice groups (groups 1, 2, 5 and 6) showed humoral immunity stimulation via antibody titration increasing, and IFN-γ and IL-2 induction. Although the cell mediated immunity was only induced in irradiated AIV (groups 1 and 5), the antibody titration and SI of splenic lymphocytes in group 4 (negative control) demonstrated no increase. Nonetheless, IO-CMC as an adjuvant makes more

stimulation in humoral and cellular immunity compared to the ISA70 oil. The immunogenicity of the irradiated AIV antigen was improved by IO NPs that were coated by CMC. Our findings revealed that the immunization of BALB/c mice with irradiated AIV-IO-CMC vaccine two times at a two-week interval could significantly elevate both cell- and antibody-mediated immunities by up-regulated antibody titration and Th-1 (IFN-γ and IL-2) and Th-2 (IL-4) cytokines, a bias towards Th1 cytokines. Furthermore, the data obtained showed that AIV-IO-CMC was effective in enhancing immunogenicity as irradiated AIV antigen administered with a clinically acceptable adjuvant (i.e. IO-CMC). HI antibody titration in the 1 and 2 groups of the vaccinated broiler chickens indicated that IO-CMC is a good adjuvant to enhance immunogenicity of irradiation-inactivated AIV antigen for inducing humoral immunity. Furthermore, the increasing of splenic lymphocyte proliferation (SI) in the 1 and 5 groups at 40th and 49th days indicated that the irradiated AIV antigen could induce the cellular immunity more than formalin-treated AIV antigen. Finally, the evaluation of AIV-IO-CMC complex for broiler chicken immunization represented further up-regulated humoral and cellular immunity in the irradiated AIV-IO-CMC group in comparison with other groups.

22126). Especially, the authors express gratitude to Dr. Hermann Unger.

ORCID

Farahnaz Motamedi-sedeh https://orcid.org/0000-0003-3388-9670
Viskam Wijewardana https://orcid.org/0000-0002-5787-8792

REFERENCES

de Abreu, F. R. & Campana-Filho, S. P. (2005). Preparation and characterization of carboxymethylchitosan. *Polímeros*, 15(2), 79–83.

Alsharifi, M., Furuya, Y., Bowden, T. R., Lobigs, M., Koskinen, A., Regner, M., Trinidad, L., Boyle, D.B., & Mullbacher, A. (2009). Intranasal flu vaccine protective against seasonal and H5N1 avian influenza infections. *Plos One*, 4(4), 1–6. https://doi.org/10.1371/journal.pone.0005336

Alsharifi, M., & Müllbacher, A. (2010). The γ-irradiated influenza vaccine and the prospect of producing safe vaccines in general. *Immunology & Cell Biology*, 88(2), 103–104. https://doi.org/10.1038/icb.2009.81

Anzai, Y. (2004). Superparamagnetic iron oxide nanoparticles: Nodal metastases and beyond. *Topics in Magnetic Resonance Imaging*, 15(2), 103–111. https://doi.org/10.1097/01.rmr.0000130602.65243.87

Asgari, S., Fakhari, Z., & Berijani, S. (2014). Synthesis and characterization of Fe3O4 magnetic nanoparticles coated with carboxymethyl chitosan grafted sodium methacrylate. *Journal of Nanostructure*, 4, 55–63.

Cristina, J., Echeverria, N., Gambaro, F., Fajardo, A., & Moreno, P. (2016). Genome-wide prediction of microRNAs in Zika virus genomes reveals possible interactions with human genes involved in the nervous system development. *bioRxiv*, 70656.

da Silva Aquino, K. A. (2012). Sterilization by gamma irradiation. *Gamma Radiation*, 9, 172–202. http://www.intechopen.com/books/gammaradiation/sterilization-by-gamma-irradiation

David, S. C., Lau, J., Singleton, E. V, Babb, R., Davies, J., Hirst, T. R., McColl, S. R., Paton, J. C., & Alsharifi, M. (2017). The effect of gamma-irradiation conditions on the immunogenicity of whole-inactivated influenza A virus vaccine. *Vaccine*, 35(7), 1071–1079.

Figuerola, A., Di Corato, R., Manna, L., & Pellegrino, T. (2010). From iron oxide nanoparticles towards advanced iron-based inorganic materials designed for biomedical applications. *Pharmacological Research*, 62(2), 126–143.

Furuya, Y., Regner, M., Lobigs, M., Koskinen, A., Müllbacher, A., & Alsharifi, M. (2010). Effect of inactivation method on the cross-protective immunity induced by whole 'killed' influenza A viruses and commercial vaccine preparations. *Journal of General Virology*, 91(6), 1450–1460.

Ghadimipour, R., Ghadimipour, I., Ameghi, A., Masoudi, S., Sedigh-Eteghad, S., & Ebrahimi, M. M. (2014). Monitoring virus harvesting time in embryonated chicken eggs inoculated with avian influenza H9N2 vaccine strain. *Archives of Razi Institute*, 69(1), 35–39.

Harris, A., Cardone, G., Winkler, D. C., Heymann, J. B., Brecher, M., White, J. M., & Steven, A. C. (2006). Influenza virus pleiomorphy characterized by cryoelectron tomography. *Proceedings of the National Academy of Sciences*, 103(50), 19123–19127.

Health, [OIE] World Organisation for Animal. (2015). Avian influenza (infection with avian influenza viruses). In *Manual of diagnostic tests and vaccines for terrestrial animals*. (1–26). OIE–World Organisation for Animal Health Paris.

Hofmann-Amtenbrink, M., Grainger, D. W., & Hofmann, H. (2015). Nanoparticles in medicine: Current challenges facing inorganic nanoparticle toxicity assessments and standardizations. *Nanomedicine: Nanotechnology, Biology and Medicine*, 11(7), 1689–1694. https://doi.org/10.1016/j.nano.2015.05.005

Khalil, A. A., Hussein, H. A., Tolba, S. K., & El-Sanousi, A. A. (2015). Preparation and evaluation of H9N2 vaccine adjuvant with Montanide ISA 71. *Global Veterinaria*, 14(5), 670–674. https://doi.org/10.5829/idosi.gv.2015.14.05.94190

Langer, R. (1990). New methods of drug delivery. *Science*, 249(4976), 1527–1533.

Marques Neto, L. M., Kipnis, A., & Junqueira-Kipnis, A. P. (2017). Role of metallic nanoparticles in vaccinology: implications for infectious disease vaccine development. *Frontiers in Immunology*, 8(8), 239. https://doi.org/10.3389/fimmu.2017.00239

Mashhadizadeh, M. H., & Amoli-Diva, M. (2012). Drug-carrying amino silane coated magnetic nanoparticles as potential vehicles for delivery of antibiotics. *Journal of Nanomedicine and Nanotechnology*, 3(4), 1–7. https://doi.org/10.4172/2157-7439.1000139

Motobu, M., El-Abasy, M., Na, K.-J., & Hirota, Y. (2002). Detection of mitogen-induced lymphocyte proliferation by bromodeoxyuridine (BrdU) incorporation in the chicken. *The Journal of Veterinary Medical Science*, 64(4), 377–379. https://doi.org/10.1292/jvms.64.377

Mourya, V. K., Inamdar, N. N., & Tiwari, A. (2010). Carboxymethyl chitosan and its applications. *Advanced Materials Letters*, 1(1), 11–33. https://doi.org/10.5185/amlett.2010.3108

Orive, G., Hernandez, R. M., Gascón, A. R., Domínguez-Gil, A., & Pedraz, J. L. (2003). Drug delivery in biotechnology: Present and future. *Current Opinion in Biotechnology*, 14(6), 659–664.

Parvin, R., Schinkoethe, J., Grund, C., Ulrich, R., Bönte, F., Behr, K. P., Voss, M., Samad, M. A., Hassan, K. E., Luttermann, C., Beer, M., & Harder, T. (2020). Comparison of pathogenicity of subtype H9 avian influenza wild-type viruses from a wide geographic origin expressing mono, di, or tribasic hemagglutinin cleavage sites. *Veterinary Research*, 51(48), 1–12. https://doi.org/10.1186/s13567-020-00771-3

Peacock, T. P., James, J., Sealy, J. E., & Iqbal, M. (2019). A global perspective on H9N2 avian influenza virus. *Viruses*, 11(7), 620–648. https://doi.org/10.3390/v11070620

Pourbakhsh, S. A., Sohraby Haghdost, I., Hablolvarid, M. H., & Gholami, M. R. (2004). Histopathological study of intratracheally inoculated

A/Chicken/Iran/259/1998 (H9N2) influenza virus in Chicken. *Archives of Razi Institute*, *58*(1), 51–62. https://doi.org/10.22092/ARI.2004.103825

Pusic, K., Aguilar, Z., McLoughlin, J., Kobuch, S., Xu, H., Tsang, M., Wang, A., & Hui, G. (2013). Iron oxide nanoparticles as a clinically acceptable delivery platform for a recombinant blood-stage human malaria vaccine. *The FASEB Journal*, *27*(3), 1153–1166.

Raie Jadidi, B., Erfan-Niya, H., & Ameghi, A. (2017). Optimizing the process of inactivating influenza virus subtype H9N2 by formalin in the production of killed avian influenza vaccine. *Archives of Razi Institute*, *72*(1), 43–49. https://doi.org/10.22034/ari.2016.107486

Reed, L. J., & Muench, H. (1938). A simple method of estimating fifty per cent endpoints. *American Journal of Epidemiology*, *27*(3), 493–497.

Reed, S. G., Orr, M. T., & Fox, C. B. (2013). Key roles of adjuvants in modern vaccines. *Nature Medicine*, *19*(12), 1597–1608. https://doi.org/10.1038/nm.3409

Salehi, B., Motamedi-Sedeh, F., Madadgar, O., Khalili, I., Ghalyan Chi Langroudi, A., Unger, H., & Wijewardana, V. (2018). Analysis of antigen conservation and inactivation of gamma-irradiated avian influenza virus subtype H9N2. *Acta Microbiologica et Immunologica Hungarica*, *65*(2), 163–171. https://doi.org/10.1556/030.65.2018.025

Sandbulte, M. R., & Roth, J. A. (2004). Methods for analysis of cell-mediated immunity in domestic animal species. *Journal of the American Veterinary Medical Association*, *225*(4), 522–530. https://doi.org/10.2460/javma.2004.225.522

Shabat, M. B., Meir, R., Haddas, R., Lapin, E., Shkoda, I., Raibstein, I., Perk, S., & Davidson, I. (2010). Development of a real-time TaqMan RT-PCR assay for the detection of H9N2 avian influenza viruses. *Journal of Virological Methods*, *168*(1–2), 72–77. https://doi.org/10.1016/j.jviromet.2010.04.019

Stauffer, F., El-Bacha, T., & Da Poian, A. T. (2006). Advances in the development of inactivated virus vaccines. *Recent Patents on Anti-Infective Drug Discovery*, *1*(3), 291–296. https://doi.org/10.2174/157489106778777673

Stear, M. J. (2005). OIE manual of diagnostic tests and vaccines for terrestrial animals (mammals, birds and bees) 5th Edn. volumes 1 & 2. World Organization for Animal Health 2004. ISBN 92 9044 622 6. *Parasitology* (727–727). Cambridge University Press. https://doi.org/10.1017/S0031182005007699

Ward, C. L., Dempsey, M. H., Ring, C. J. A., Kempson, R. E., Zhang, L., Gor, D., Snowden, B. W., & Tisdale, M. (2004). Design and performance testing of quantitative real time PCR assays for influenza A and B viral load measurement. *Journal of Clinical Virology*, *29*(3), 179–188. https://doi.org/10.1016/S1386-6532(03)00122-7

Whitby, J. L., & Gelda, A. K. (1979). Use of incremental doses of cobalt 60 radiation as a means to determine radiation sterilization dose. *Journal of the Parenteral Drug Association*, *33*(3), 144–155.

WHO. (2013). *Laboratory Procedures Serological detection of avian influenza A (H7N9) virus infections by turkey haemagglutination-inhibition assay*. WHO Collaborating Center for Reference and Research on Influenza Chinese. http://www.who.int/influenza/gisrs_laboratory/cnic_serological_diagnosis_hai_a_h7n9.pdf

Xie, Y. H., Zhang, Y. T., Huang, X. Z., Ding, Y. H., & Huang, L. P. (2014). Preparation of carboxymethyl chitosan magnetic nanoparticles and separation of Chinese medicines components. *Advanced Materials Research*, *936*, 304–309.

Xu, H., Aguilar, Z. P., Su, H., Dixon, J., Wei, H., & Wang, A. (2009). Breast cancer cell imaging using semiconductor quantum dots. *ECS Transactions*, *25*(11), 69–77.

Xu, H., Aguilar, Z. P., & Wang, A. (2010). Quantum dot-based sensors for proteins. *ECS Transactions*, *25*(31), 1–8.

Xu, H., Wei, H., Aguilar, Z.P., Waldron, J.L., Wang, A.Y. (2009). Application of semiconductor quantum dots for breast cancer cell sensing. Biomedical Engineering and Informatics, BMEI '09. *The 2nd International Conference on BioMedical Engineering and Informatics (BMEI)*, Tianjin, China. https://doi.org/10.1109/BMEI.2009.5305551